Accepted for publication in Energy and Buildings

https://doi.org/10.1016/j.enbuild.2020.110488

On the resistance to heat flow across soil-structure interfaces

AUTHORS:

Bourne-Webb, P.J. [a]

peter.bourne-webb.co.uk@tecnico.ulisboa.pt

de Sousa Figueira, J.D. [a]

joao.figueira@tecnico.ulisboa.pt

Bodas Freitas, T.M. [a]

teresabodas@tecnico.ulisboa.pt

[a] CERIS, DECivil, Instituto Superior Técnico, Universidade de Lisboa, Lisboa, Portugal

ABSTRACT:

A number of recent publications have suggested that in order to reproduce thermal testing of energy piles, a finite value for the geo-contact thermal resistance (geo-CTR) at the soil-structure interface needs to be introduced. There is currently no guidance as to what value the geo-CTR should have. The geo-CTR will have two potential impacts in terms of the use of energy geo-structures, (i) reducing heat exchange efficiency, and (ii) increasing temperature changes and associated mechanical impacts within the geo-structure. This article sets out a new experimental method for quantifying the geo-CTR. The proposed method is based on the imposition of a heat flux through the two solid materials that form the contact. Its novelty rests with the acknowledgement that heat loss is inevitable and that the geo-CTR can be more reliably defined based on heat flow measurements at the actual contact. This concept is demonstrated via numerical modelling of a generic test set-up, where the errors induced by not accounting for heat loss, the interpolation of temperatures to the contact and the presence of the heat flow sensor were assessed. Initial test results are then presented that demonstrate how the method works. These results suggest that for a dry medium sand, while the geo-CTR is sensitive to the soil density, it is small and the effect on heat transfer is also likely to be small. Further testing will explore the relative importance of a number of factors and in particular, the soil type, on the geo-CTR.

KEY WORDS: contact resistance; energy geostructure; geotechnics; heat transfer; laboratory test

1. INTRODUCTION

When heat flows between two differing solid materials in contact with each other, there will be a finite contact thermal resistance (CTR) developed at the interface which is influenced by amongst other things geometric irregularities, surface micro-hardness, surface cleanliness, contact pressure, thermal conductivity of the solids at the contact and interstitial materials, Yovanovich (1999) [1]. Typical values for the CTR on ceramic-ceramic interfaces lie in the range of 0.0003 to 0.002 m^2K/W (Yovanovich, 1999) [1]; on rough metal-metal surfaces it may be similar or even higher, while on smooth metal-metal interfaces it can be an order of magnitude lower.

The range of likely values for CTR are such that its effect is likely to be small for insulators whose thermal resistance is many orders of magnitude greater but is significant for metals whose thermal resistance is similar to measured values of CTR. Materials associated with geo-heat exchange (e.g. soil, rock, grouts and concrete) offer thermal resistance values between those of insulators (1-2 orders of magnitude greater) and metals (1-2 orders of magnitude lower), and it is not immediately apparent if the CTR effect is significant for geo-heat exchange systems or not. In principle, while the scale is different the same factors as described above will affect geo-contacts – geometric irregularities will occur depending on how the geo-structure is constructed in the ground, there will be a variety of differing contacts (particle-particle, cement paste-particle) and depending on the soil density and confining pressure, varying proportions of voids, which maybe be dry (air filled voids), partially saturated or fully saturated with water, or other fluids and gases.

In borehole heat exchangers, the borehole is modelled as a lumped resistance which includes the effect of the constituent materials and their contacts, within the heat exchanger system, Beier & Smith (2002) [2]. When it comes to geo-structures, the situation is more complex; a lumped resistance approach may be able to be used for piles but for planar structures such as walls, such an approach may no longer be reasonable. Geo-contact thermal resistance (geo-CTR) will have two impacts in the operation of energy geo-structures: reduced heat exchange efficiency, and increased temperature changes with associated mechanical impacts within the geo-structure.

Svec et al. (1983) [3] investigated the heat exchange between plastic pipes of varying configuration and a saturated clay soil using a benchtop testing apparatus. Based on a comprehensive set of observations, Figure 1, they were able to evaluate the thermal resistance of the various components, including the pipe-soil geo-CTR, R_{int}, for which values in the range of 0.19 to 0.45 m.K/W (0.003 to 0.007 m^2K/W) associated with temperature drops, ΔT_{int} of 0.3 °C to 0.7°C, were obtained. Differences in the geo-CTR between heating and cooling were noted and attributed to the differing thermal expansion properties of the soil and tube. The results presented by Svec et al. (1983) [3] suggest that the geo-CTR may represent 5% to 10% of the total thermal resistance of a borehole heat exchanger.

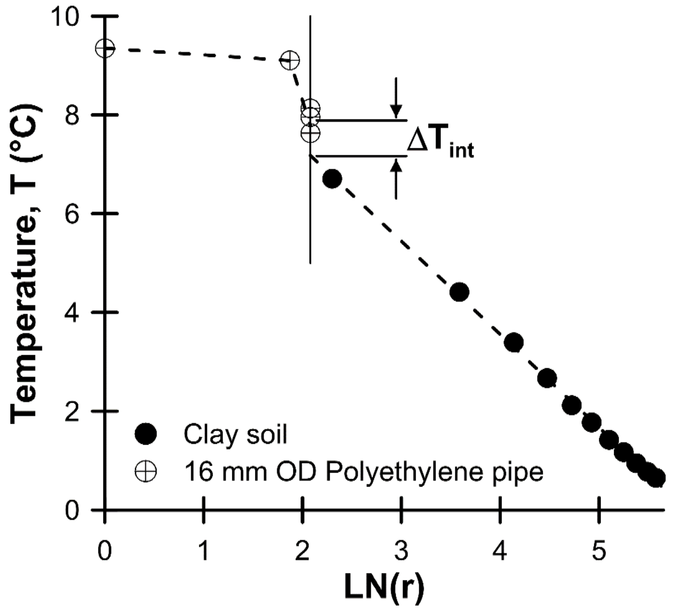

Figure 1. Radial temperature variation through polyethylene pipe embedded in clay, from Svec et al. (1983) [3]

Hellstrom (1991) [4] recognised that heat transfer between the heat exchanger and the surrounding ground involves geo-CTR. However, rather than being an intrinsic property of the interface, it is attributed to ill-fitting borehole liners leaving an irregular contact with the surrounding ground. The geo-CTR is then identified as being a function of the characteristic thickness of the surrounding gap and the thermal conductivity of the in-fill material. Wang et al. (2016) [5] develop a theoretical model for evaluating the impact of geo-CTR on the heat loss performance in heavy-oil well bores. As with Hellstrom (1991) [4], they ascribe this resistance to irregularities in the contact between the natural ground and the grout body within the well bore. Wang et al. (2016) [5] then apply this model to the back-analysis of field data and demonstrate that in this instance, the geo-CTR effect may be significant.

In studies modelling heat flow from buildings to the ground, varying assumptions seem to be made regarding the geo-CTR; either it is ignored (zero geo-CTR) or a finite value used. When ignored, the assumption regarding the geo-CTR is usually not stated explicitly. Thomas & Rees (1999) [6] used a value of 0.04 m^2K/W which is taken from ISO 6946 (2007) [7] but this corresponds to an air-surface contact with an air flow velocity of 4 m/s, and its use was not discussed. Al-Temeemi & Harris (2003) [8] used a value of 0.005 m^2K/W recognising that there will be some geo-CTR at the soil-structure interface and it is likely to be lower than that of an external air-contact surface, but no further justification was given.

More recently, in the back-analysis of thermal response tests on energy piles, Qi (2015) [9] has suggested geo-CTR values in the range of 0.25 m^2K/W (cooling) and 0.17 m^2K/W (heating), while Cecinato et al. (2016) [10] resorted to a fictional "air gap" of 1 cm thickness, equivalent to a geo-CTR of 0.35 m^2K/W, in order to reproduce thermal response tests. Although it should be borne in mind that these values are arrived at from back-analysis and will depend on many other assumptions regarding inputs in the respective analyses, the reported values suggest that the CTR in geo-heat exchange problems may be significant. Not accounting for this effect may impact on the reliability of thermal and thermo-mechanical analysis, and perhaps the sustainability of heat exchange via energy geostructures.

Freitas Assunção (2014) [11] examined the impact of varying the geo-CTR on a pile-soil interface and Figure 2 shows how in the case examined, for the range of geo-CTR values discussed above, temperature change and heat flow across the pile-soil interface will change very quickly should the geo-CTR increase beyond about 0.04 m^2K/W.

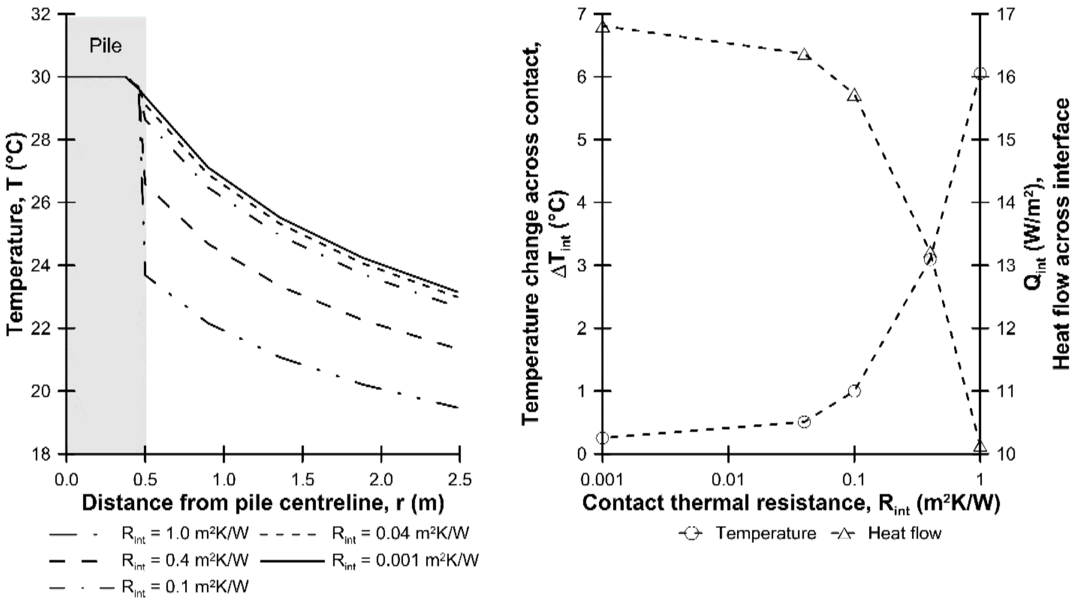

Figure 2. Effect of geo-contact thermal resistance on energy pile heat transfer, after [11]

In this paper, the basis for a new laboratory test method to evaluate the geo-contact thermal resistance (geo-CTR) is described and evaluated alongside generic numerical analysis of the problem, undertaken as part of the development of the test procedure. Subsequently, initial testing results for a geo-contact between a fine sand at two different states of compaction and a limestone aggregate based concrete are presented to demonstrate the application of the method for determining geo-CTR in practice.

2. Geo-CTR TEST METHODOLOGY

2.1. General

The test method employed has been scaled up from methods employed for obtaining the contact thermal resistance across metal-to-metal contacts, e.g. Xian et al. (2018) [12] and Madhusudana (2000) [13]. Existing test procedures set-out to establish one-dimensional (no heat loss), approximately steady-state heat flow across two samples, then temperature measurements along the sample centreline are extrapolated to the contact to obtain the change in temperature at the contact (ΔT_{int}), and an average heat flux through the samples (typically obtained from meter-bars at each end) is used as a measure of the heat flux at the contact (q_2). The CTR is then estimated through Equation (1),

$$R_{int} = \frac{\Delta T_{int}}{q_2} \quad (1)$$

Xian et al. (2018) [12] identify these steady-state methods as being the most appropriate for bulk materials.

Figure 3 provides a schematic layout of such a test modified for the current application; a concrete sample and soil sample are contained within a PVC tube which itself will be contained within a larger enclosure that provides support and additional thermal insulation. The test procedure is as follows:

1. Heat is applied at the base of the concrete sample through a heating pad and the input heat flux (q_1) and temperature (T_0) are recorded by a thin-film heat flux sensor) with an integrated Type-K thermocouple temperature sensor (HFS1 & TS0);
2. Along the centreline of the samples, the temperature is continuously recorded at various points by temperature sensors (TS1 to TS6)
3. The heat flux (q_2) across the concrete-soil interface (geo-contact), is measured with a second thin-film heat flux sensor (HFS2 & TS7);
4. The temperature variation through each material (T_1 to T_3 and T_4 to T_6, in the concrete and soil samples respectively) is plotted and extrapolated to the geo-contact (Figure 3), from which it is possible to estimate the change in temperature across the geo-contact (ΔT_{int});
5. Having determined ΔT_{int} and using the measured q_2 values, the geo-CTR can be estimated through Equation (1).

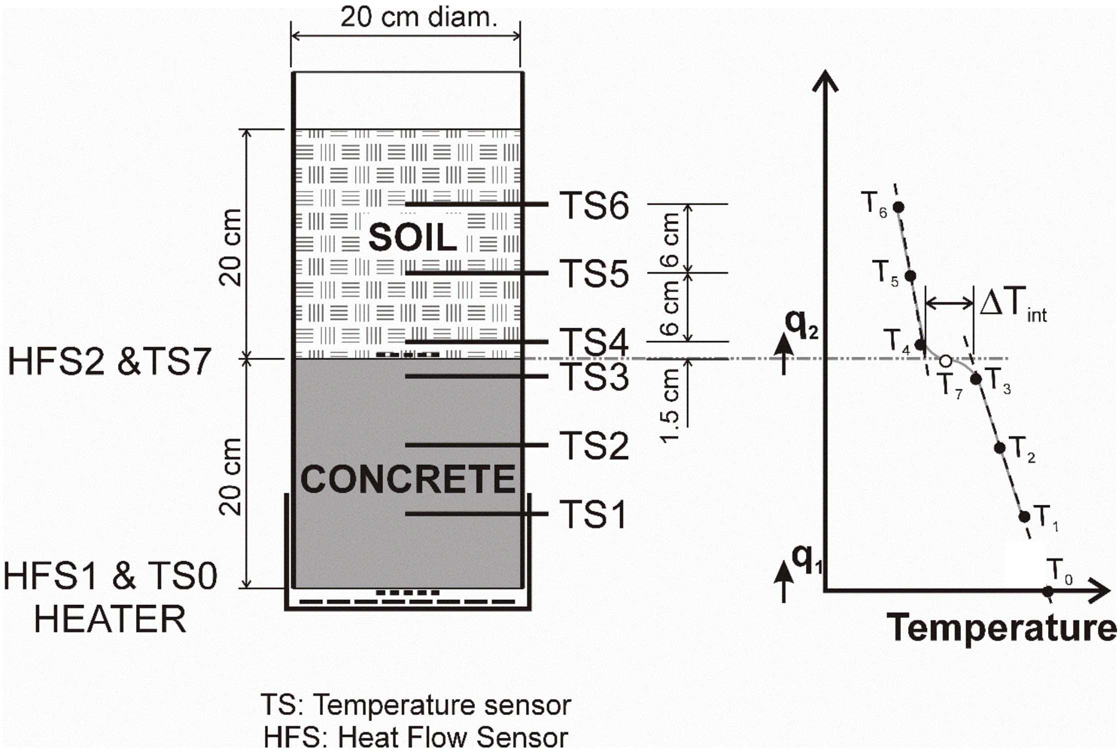

Figure 3. Schematic layout of geo-contact thermal resistance test

The key to the test methodology propose in this paper is the inclusion of a thin-film heat flow sensor at the interface (HFS2, Figure 3). This sensor was added as it was recognised that heat flow is not one-dimensional and not considering radial heat losses would lead to significant errors in the derived CTR, Madhusudana (2000) [13]. Low et al. (2017) [14] confirm the short comings of assuming a one-dimensional heat flow mechanism in thermal cell measurements of soil thermal conductivity. Further, Mondal et al. (2016) [15] used multiple heat flow sensors embedded in the soil sample to compensate for heat losses when determining the thermal conductivity of soils in a thermal cell.

In principle, the interpretation of the geo-CTR test could also be undertaken using inverse heat conduction analysis, however this is not as straightforward as it would first appear as the heat flow problem is not one-dimensional due to the heat losses, which is the usual assumption in reported application of this technique, Asif et al. (2019) [16], Shojaeefard et al. (2009) [17], and as a consequence there are a multitude of parameters and boundary conditions that are not well defined. An approach for inverse-analysis of the tests is in development, and may result in the need for additional heat flow and/or temperature measurements during the test to ensure accurate numerical modelling.

Prior to constructing the test rig, a number of numerical analyses were undertaken in order to understand where heat was flowing in the test specimen and whether reliable results could be obtained; these are described in the following section before detailing the test set-up and procedures.

2.2. Numerical analysis of Geo-CTR tests method

2.2.1. Basis for analyses

Before setting up the testing equipment, the principles of the test method were investigated by means of transient thermal analysis carried out with the commercial finite element analysis software ABAQUS Standard 2016. Two axisymmetric model geometries were considered:

1) The first considered perfect axial heat flow through the two conducting materials: concrete and soil, with adiabatic side boundaries ensuring no radial heat losses, Figure 4(a). The objective of the analyses made with this model was to provide a comparison with the case where heat losses were considered. The cases analysed differed in how the soil-air surface boundary condition was specified, i.e. Case A: Constant temperature (20°C) and Case B: Convection boundary conditions with a surface conductance, h = 10 W/m^{2}K and an air temperature of 20°C. The thermal conductance value of 10 W/m^{2}K used for the upper surface boundary condition is considered representative of the likely value and includes a thermal radiation component, Figure 5.
2) From the outset, it was recognised that radial heat losses were inevitable and so as to be able to understand the impact of these losses, analyses were undertaken based on what were considered realistic material properties and boundary conditions, and a Case C model representing the proposed test set-up was developed based on Figure 4(b).

Figure 4 shows a schematic of the finite element models including the assumed boundary conditions, and a table that details the thermal properties adopted for each of the materials modelled. All the materials (soil, concrete and contact) were characterised by bulk thermal properties which are assumed to be temperature and pressure independent. This is considered reasonable given the range of temperature and confining pressure considered in the analysis. The finite element mesh was generated using quadrilateral 4-node linear finite elements with three differing mesh densities, Mesh 1: 10 mm x 10 mm, Mesh 2: 5 mm x 5 mm and Mesh 3: 2.5 mm x 2.5 mm. It should be noted that these analyses were based on a set of generic material thermal properties and boundary conditions, with the aim of evaluating various aspects of the proposed test methodology, and were not intended to represent the tests presented later.

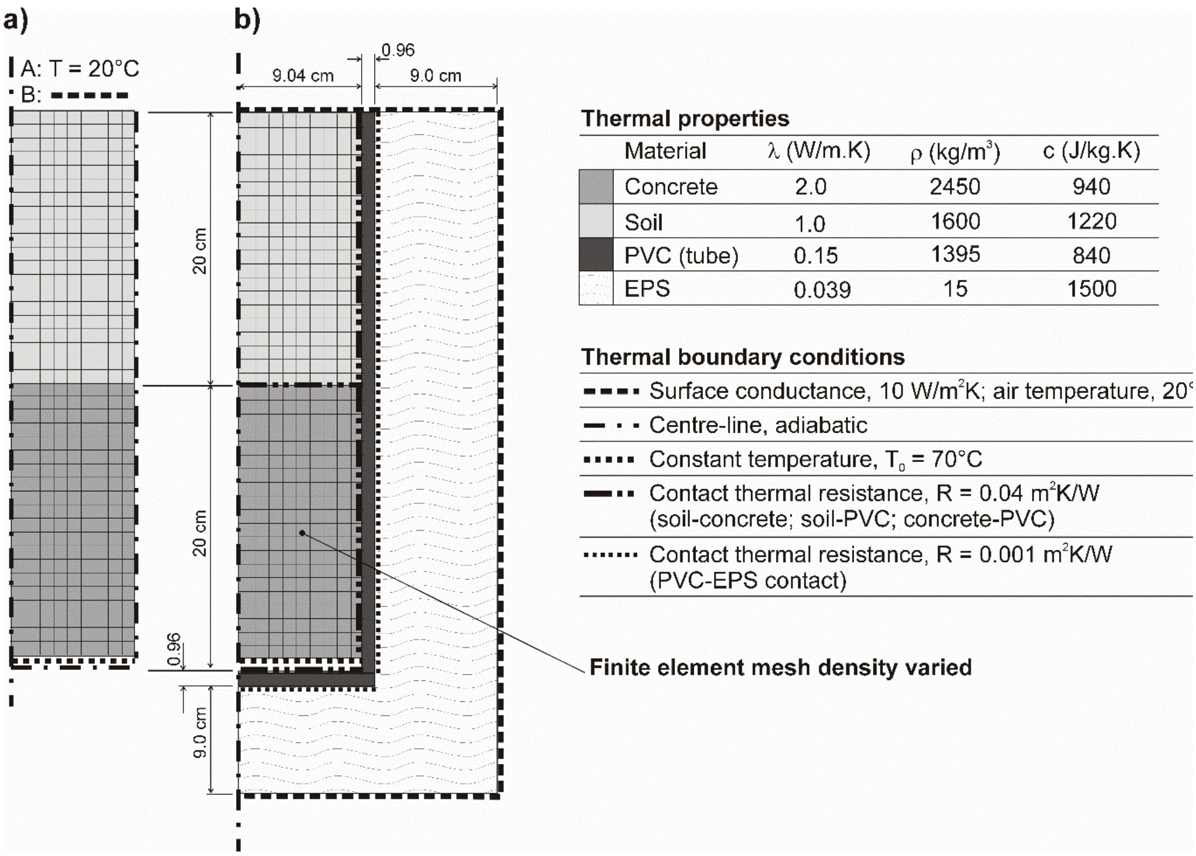

Figure 4. Schematic of finite element model geometry

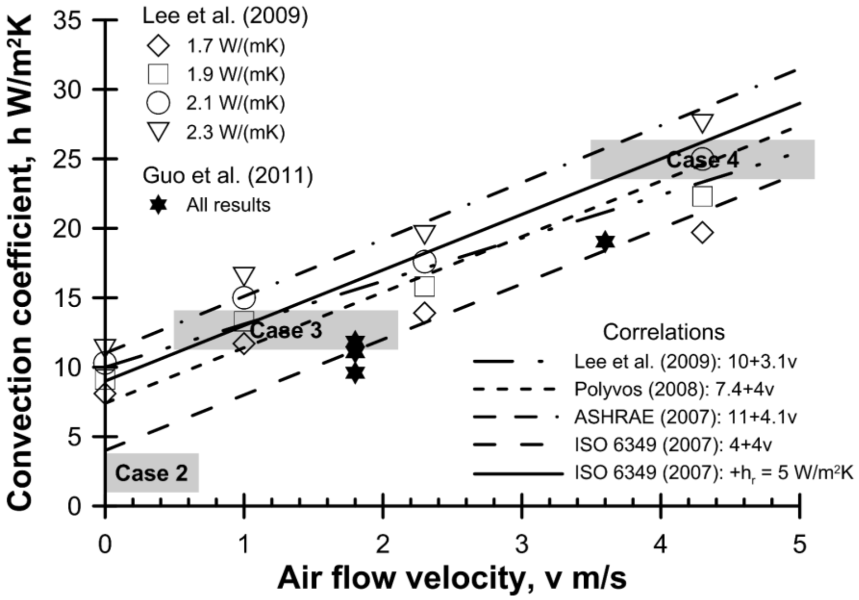

Figure 5. Comparison of correlations for forced convective heat transfer coefficient, Bourne-Webb et al. (2016) [18]

2.2.2. Heat flow through the test elements

Figure 6 illustrates for Case C, a) the evolution of temperature at key points along the test sample's centreline as the test proceeds, and b) the temperature distribution along the axis of the model at various times during the test. It is apparent that the heat flow approaches a steady-state condition after about 2 days. The temperature distribution from Cases A and B at 6 days are also shown in Figure 6(b); the absolute values along the profiles differ due to the different boundary conditions assigned at the upper soil-air surface, however, either side of the interface, the temperature variation is linear. In contrast, in Case C, lateral heat loss led to larger temperature drops across the concrete and soil, and a nonlinear variation in temperature along the sample, even when close to steady-state conditions were achieved.

The temperature drop across the interface, ΔT_{int} predicted in each of the analyses is illustrated in Figure 7(a). Given that in the three analyses, the same geo-CTR is assumed, it is clear that the change in temperature recorded across the contact also depends on the other imposed boundary conditions. In Figure 6, to either side of the contact between the concrete and the soil, it is apparent that the temperature gradient in Case A is larger than in B; the heat flow is therefore higher and thus, for a given CTR, the temperature drop must be larger. The gradient in the temperature profile in Cases B and C are similar and flatter, which is why the temperature drop is smaller.

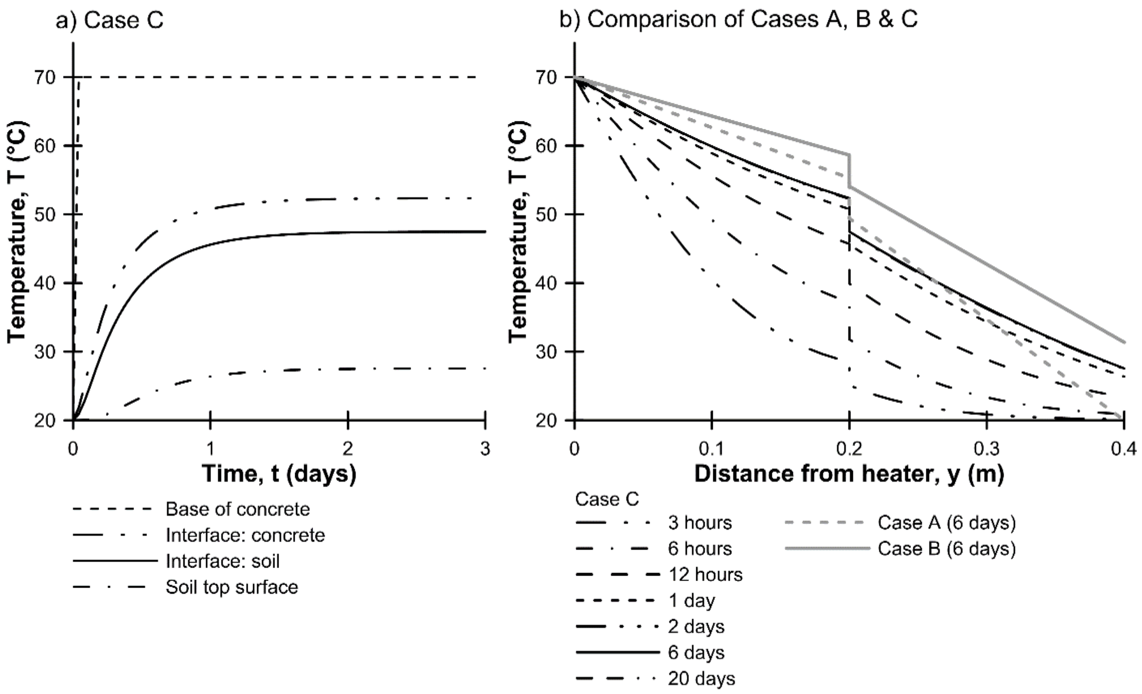

Figure 6. Evolution of centre-line temperatures

Figure 7(b) shows the relative error in the estimation of the geo-CTR by application of Equation (1), based on the temperature drop in Figure 7(a) and using the input heat flux q_1 from the base of the concrete (Figure 3). In Cases A and B, the relative error approached zero between 2 to 3 days after heating started. However, in Case C the relative error remains about 10%. This is a direct consequence of the heat losses occurring between the base of the sample and the interface, which leads to the input heat flux, q_1 not being representative of the heat flux at the contact.

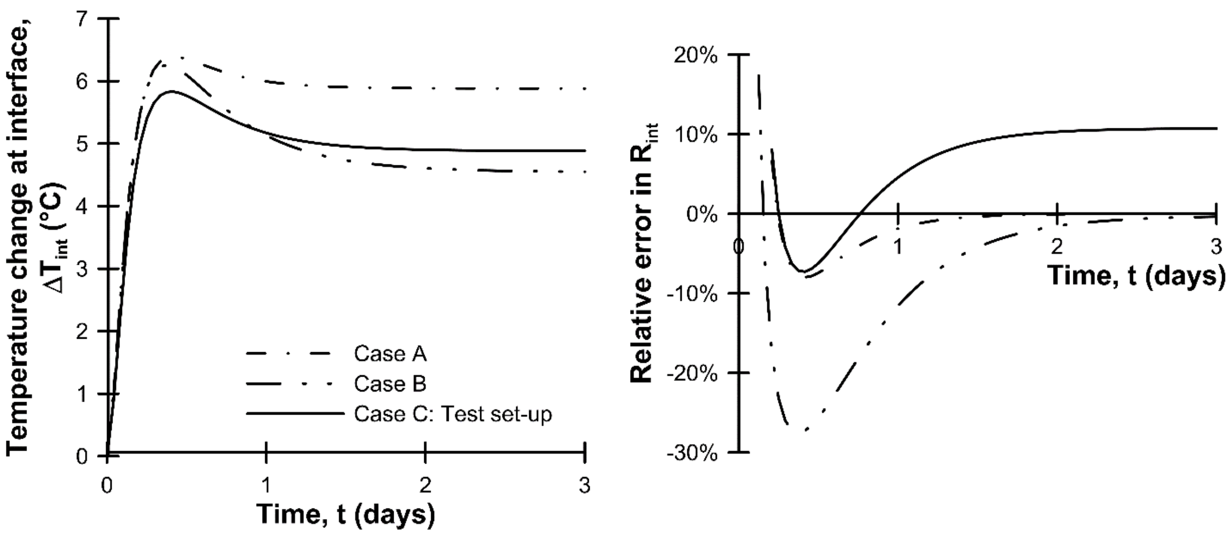

Figure 7. a) Evolution of temperature change across Geo-contact and b) Relative error in evaluation of Geo-CTR when using constant input flux, q_1 at base of test sample

This discrepancy in the estimation of the geo-CTR resistance was resolved by the use of the heat flux at the interface, q_2 (Figure 3). Due to the heat losses, the value of q_2 in Case C, was about 9% lower than in the idealised Case B, and the relative error quickly reduces to a residual value of 0.7%, Figure 8. This confirms the need for direct measurement of the heat flux across the interface in order to obtain a reliable estimate of the geo-CTR.

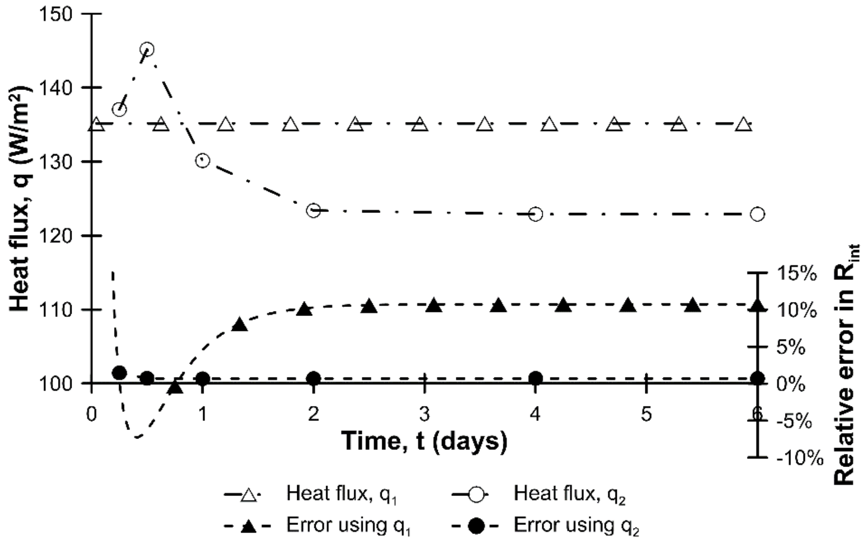

Figure 8. Effect of location of heat flux measurement on the evaluation of geo-CTR (Input heat flux, q_1; Interface heat flux, q_2 see Figure 3)

To investigate this residual error value further, the finite element mesh was refined in the vicinity of the geo-contact. It was found that in terms of the temperature variation on the centreline across the interface, this had an insignificant effect but as Figure 9 illustrates, the axial heat flux altered as the finite element mesh moved from being a relatively coarse mesh (Mesh 1) to a succession of refined meshes (Mesh 2 and 3). The changes in predicted heat flux at the geo-contact led to a reduction in the residual error from 0.7% to 0.2%. It was concluded that the major source of the residual error was due to the finite element model, rather than inherent problems in the test set-up and confirmed that it is crucial to have a heat flow measurement at the interface.

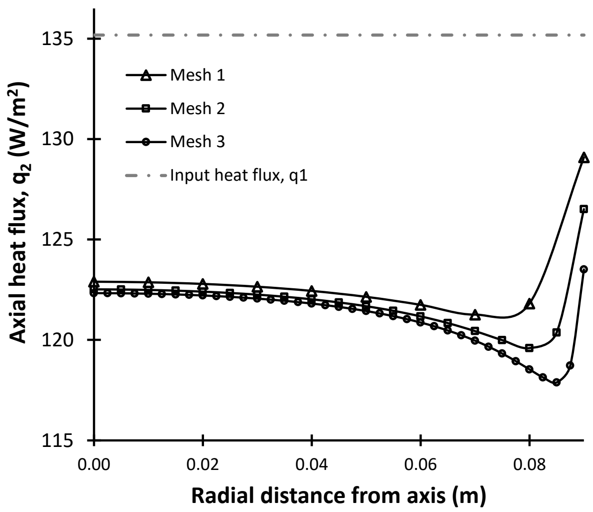

Figure 9. Impact of mesh refinement on radial distribution of axial heat flux at Geo-contact

2.2.3. Interpolation of temperatures to geo-contact

In the test apparatus, it will not be possible to have continuous temperature profiles along the sample axis and the planned configuration is to have three measurement points. The first, about 1 to 2 cm from the geo-contact, and the remainder at a spacing of several centimetres, Figure 3. Therefore, the numerical analysis results have been examined in order to see how the measurement locations impact on the reliability of the inferred geo-contact thermal resistance estimate.

Figure 10 illustrates the interpolation through three sample points either side of the interface, at distances approximating those above, to obtain the interpolated contact temperatures, $T_{1,extr}$ and $T_{2,extr}$ and Table 1 summarises the resulting estimates for R_{int} and its relative error at different times. A quadratic function was used to extrapolate the data to the contact and beyond Day 2, the results are largely indistinguishable. Though not shown here, different simple extrapolation functions were considered but the quadratic interpolation was found to provide a better fit, leading to relative errors of around 1%, which seems satisfactory.

The effect of temperature measurement location was also investigated by considering that these started closer to the geo-contact. This was found to lead to an improvement in the relative error in geo-CTR by about 0.1%. To conclude, the relative error in the estimation of geo-CTR due to the extrapolation of the contact temperatures from discrete temperature measurements within the solid materials using a simple quadratic function, is expected to be less than about 1%. As noted earlier, the interpretation of the geo-CTR test could also be undertaken using inverse heat conduction analysis, and this aspect of the test interpretation is under development.

Table 1 highlights a further advantage of incorporating the heat flux measurement at the interface, i.e. the evaluation of the interface resistance can be made with almost equal reliability without the system having to reach a steady-state condition, i.e. the interface resistance inferred from extrapolated results does not change significantly after about half a day of heating.

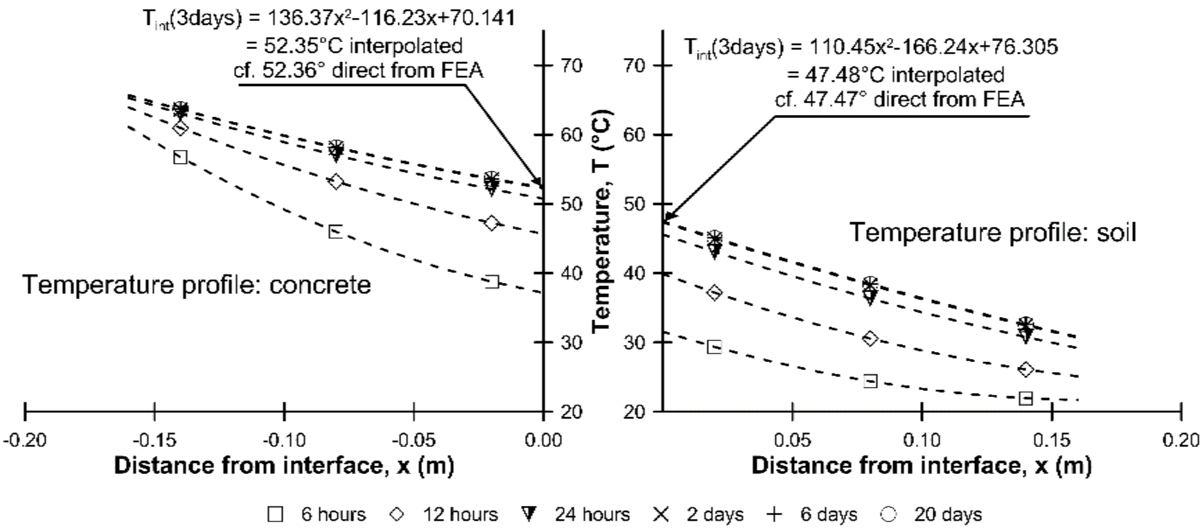

Figure 10. Interpolation of interface temperature from sample points in numerical model, 2 cm, 8 cm and 14 cm either side of geo-contact and at different times after heating commences.

Table 1. Reliability of geo-CTR from extrapolated point temperature measurements

Source	Time (days)	$T_{1,extr}$ (°C)	$T_{2,extr}$ (°C)	ΔT_{int} (°C)	q_2 (W/m_2)	R_{int} (m^2K/W)	Rel. error (%)
Quadratic extrapolation	0.25	37.15	31.55	5.59	137.1	0.0408	1.97%
	0.50	45.65	39.88	5.77	145.2	0.0397	0.64%
	1	50.75	45.59	5.15	130.1	0.0396	1.01%
	2	52.25	47.36	4.89	123.4	0.0396	0.91%
	3	52.35	47.48	4.87	123.1	0.0396	1.01%
	6	52.35	47.49	4.87	122.9	0.0396	0.96%
	20	52.36	47.48	4.87	122.9	0.0396	0.91%
FEA at interface	20	52.37	47.48	4.88	122.9	0.0397	0.70%

2.2.4. Influence of heat flow sensor resistance

The heat flow sensor is 38.1 mm x 28.5 mm x 0.18 mm thick and presents a finite thermal resistance of about 0.0018 m^2K/W and thus, will impact the flow of heat through the sample. Therefore, an additional set of analyses were undertaken where the thermal resistance across central part of the geo-contact (to a radius of 18 mm giving an equivalent sensor area of c. 1000 mm^2) was increased to (R_{int} + 0.0018) m^2K/W and where R_{int} was assigned values of 0.4, 0.04 and 0.004 m^2K/W. As the geo-CTR was reduced from 0.4 to 0.04 and then 0.004 m^2K/W, the effect of the sensor was found to introduce an apparent error in the geo-CTR of 0.3%, 2.3% and 4.7% respectively. As expected, if the sensor resistance is similar to the geo-CTR, then its effect on the overall resistance is greater and the error in estimating the contact thermal resistance increases. However, as noted earlier when the CTR is less than about 0.04 m^2K/W, the effect of CTR on heat flow is likely to be small (Figure 2) and thus, any errors in its measurement will not be important.

3. Geo-CTR TEST METHOD: PROOF OF CONCEPT

3.1.1. Configuration

In the development of the final test configuration, the basic element dimensions indicated in Figure 3 were retained, i.e. 20 cm diameter and 20 cm high soil and concrete specimens contained in a PVC pipe. The final test configuration includes a wooden box clad with 10 mm plywood which was used to support the tube, and the void around the tube is filled with expanded polystyrene (EPS) packaging chips in order to provide insulation and to minimise convection within the void.

A 20 cm diam. class SN2 un-plasticized polyvinyl chloride (uPVC) tube with a nominal wall thickness of 3.9 mm was used to contain the soil and concrete specimens. The bottom end of the tube was supported in a compatible end cap within which the heat source (180 mm diam., 385 W silicone pad heater) and heat flux sensor (HFS1) with integrated thermocouple were also contained. The HFS is a self-generating thermopile type transducer with a sensitivity of 2.06 $\mu V/(W/m^2)$ which was sourced from Omega® Engineering.

The heat input is managed using an electronic PID controller based on the temperature recorded at the thermocouple (TS0, Figure 3) integrated in HFS1 next to the heating pad. The set-point temperature in the controller was set to ramp to a value of 75°C (as measured by TS0) at 1°C/minute (from an initial temperature of 19-20°C), after which it was maintained to within ±0.5°C by the controller. It should be noted that because the controller was switching the heat pad on and off to maintain the set-point, the heat flux at the base of the concrete was highly variable. However, this quantity is not needed for the interpretation of the geo-CTR. Future tests will use a rheostat type switch to control the heat flux rather than the temperature.

Ruggedized thermocouples (Type K) were embedded in the soil and concrete specimens, symmetrically about the interface between the two materials and with the sensor tip located on the sample centreline, as indicated in Figure 3. The thermocouples were fitted through holes drilled in the wall of the tube, supported with rubber grommets. The surfaces of the thermocouples in contact with the concrete were coated with thermal grease, to ensure good thermal contact and to aid in releasing the thermocouples for re-use in other tests.

Finally, HFS2 with an integrated thermocouple was located on the interface. As demonstrated in the previous section, this configuration was necessary if reliable geo-CTR values were to be obtained. During the test, all data from the HFS and TS were captured via a 16-Channel Data Acquisition system (GW Instruments, iNET-555) and recorded on a desktop computer.

3.1.2. Materials

The concrete used had a 28 day compression strength of 30 MPa, a water cement ratio of 0.52, a ratio of cement to sand to coarse aggregate of 1.0:2.0:2.6, and used limestone aggregates. The concrete was placed carefully in the tube so as not to disturb the thermocouples, and was vibrated to help remove entrained air pockets. The concrete was then allowed to moist cure in the tube for around a month. The soil infill used in the preliminary testing was a dry, uniform, medium to coarse silica sand with a mean particle size, D_{50} of about 0.6 mm. Minimum and maximum dry density values of 1.34 and 1.58 g/m^3 were obtained.

3.2. Initial results

3.2.1. Test 1: Loose sand

In this test, the sand was poured into the tube with minimal compaction. Figure 11(a) and (b) illustrate the evolution of the temperatures recorded by the thermocouples (open symbols), and the interpolated temperature profile along the sample centreline (dashed lines) in the concrete and loose sand respectively. The evolution of the temperature difference at the contact and the contact heat flux are shown in Figure 11(c), and Figure 11(d) shows the evolution of the inferred geo-CTR. In Figure 11(a) it is apparent that the temperatures in the concrete if extrapolated closer to the base (x = -0.2 m) will not reach 70°C. This was attributed to either a poor contact between the concrete and the heater pad and/or non-uniformity in the concrete sample (e.g. segregation of aggregates and cement). The arrangements for setting the heating pad against the concrete were improved in the dense sand tests and further modified for future testing to address this.

The results of this test are also summarized in Table 2. It is apparent that the method does not arrive at a value for the geo-CTR that has a level of uncertainty as small as that suggested by the numerical analysis. However, after 24 hours, the value is stable to within 10% of the value at 45 hours which is satisfactory.

Table 2. Inferred concrete-soil contact thermal resistance from Test 1 measurements

Source	Time (Hours)	$T_{1,extr}$ (°C)	$T_{2,extr}$ (°C)	ΔT_{int} (°C)	q_2 (W/m^2)	R_{int} (m^{2}K/W)	%-error[(1)]
Quadratic extrapolation	2	24.97	23.69	1.28	28.7	0.045	123
	4	32.63	30.85	1.78	66.7	0.027	33
	6	38.91	37.49	1.42	72.0	0.020	-1
	12	47.59	44.74	0.85	53.2	0.016	-20
	18	49.96	49.26	0.70	42.2	0.017	-17
	24	50.68	49.99	0.69	38.1	0.018	-9
	36	51.11	50.44	0.67	36.1	0.019	-7
	45	51.04	50.31	0.72	36.1	0.020	-

[(1)] Relative error is with respect to value at 45 hours

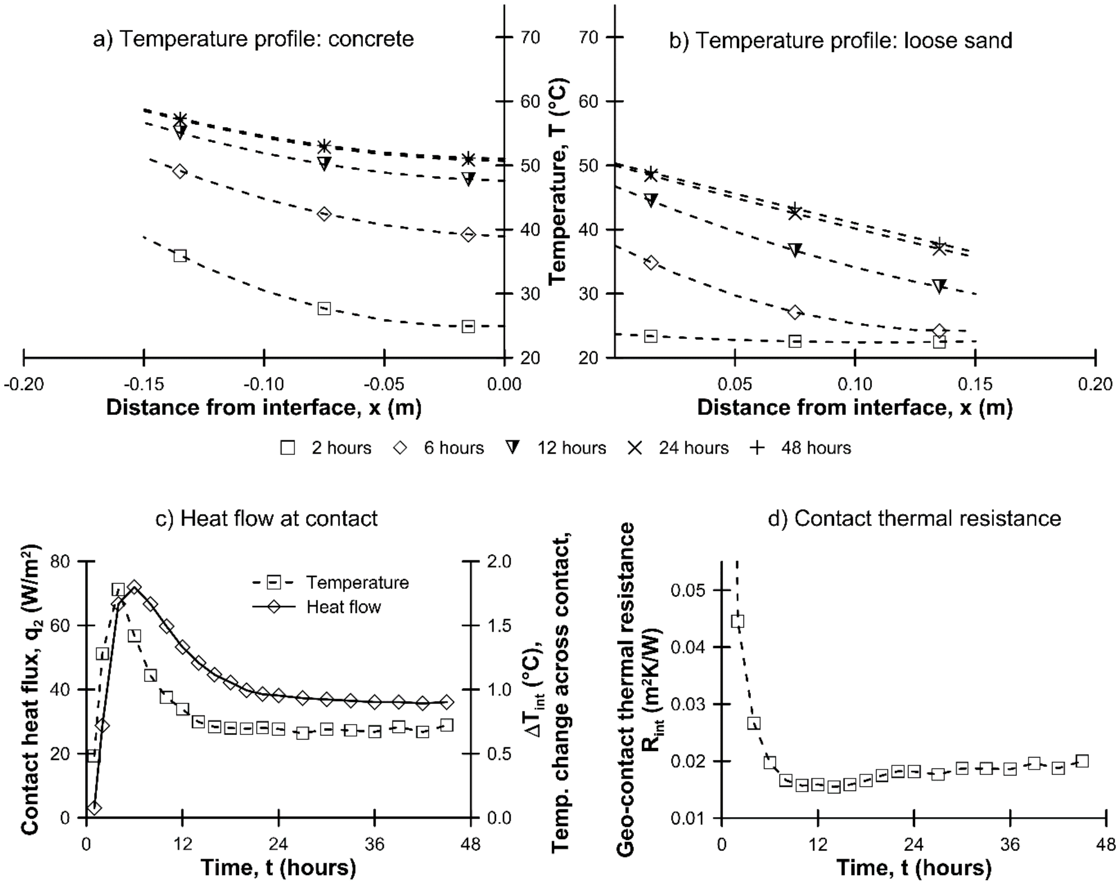

Figure 11. Temperature & heat flux measurements during Test 1

3.2.2. Test 2: Dense sand

In this test, the sand was placed in layers several centimetres thick to which 20 blows of a 5.58 kg hammer with a diameter of 100 mm, falling a height of about 5 cm were applied to produce a dense sand sample. Figure 12(a) and (b) illustrate the evolution of the temperatures recorded by the thermocouples (open symbols) and the interpolated temperature profile (dashed lines). The evolution of the temperature difference at the contact and the measured contact heat flux are shown in Figure 12(c), and Figure 12(d) shows the evolution of the inferred geo-CTR.

The results of this test are summarized in Table 3. As seen in the test on loose sand, it is apparent that the method does not arrive at a value for the geo-CTR that has a level of uncertainty as small as that suggested by the numerical analysis. However, after 24 hours, the value is stable to within 10% (of the value at 48 hours) which again, is satisfactory.

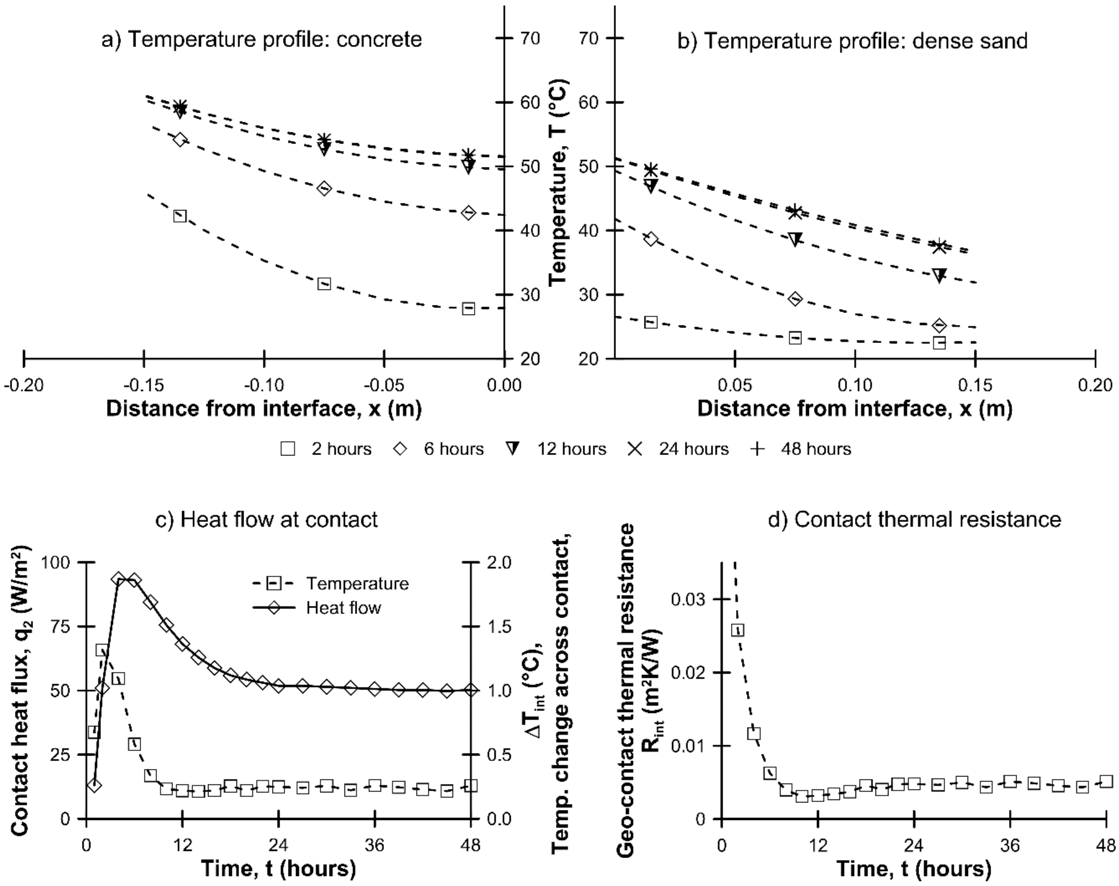

Figure 12. Temperature & heat flux measurements during Test 2

Table 3. Inferred concrete-soil contact thermal resistance from Test 2 measurements

Source	Time (Hours)	$T_{1,extr}$ (°C)	$T_{2,extr}$ (°C)	ΔT_{int} (°C)	q_2 (W/m²)	R_{int} (m²K/W)	%-error(1)
Quadratic extrapolation	2	27.9	26.6	1.32	51.0	0.026	400
	4	36.5	35.4	1.09	93.5	0.012	128
	6	42.4	41.8	0.582	93.1	0.0063	22
	12	49.5	49.3	0.219	68.2	0.0032	37
	18	51.2	50.9	0.256	55.9	0.0046	11
	24	51.5	51.2	0.249	51.9	0.0048	6
	36	51.7	51.4	0.259	50.6	0.0051	0
	48	51.6	51.3	0.258	50.2	0.0051	-

(1) Relative error is with respect to value at 48 hours

3.2.3. Discussion

It is apparent from the results of these two tests that the geo-CTR is sensitive to the density of the sand, and a reduction from the loose to dense sand sample of 0.02 to 0.005 m^2K/W. This is to be expected as a higher density equates to more particle contacts, less air voids and therefore more efficient heat flow across the geo-contact. With minimum and maximum dry density values of 1.34 and 1.58 g/m^3 respectively, the maximum possible increase in dry density was about 20%. However, a four-fold reduction in the geo-CTR as the density increased was recorded in this case. To highlight the sensitivity of the soil thermal properties with respect to dry density, it is noted that Alrtimi et al. (2016) [19] report an increase in the thermal conductivity of a dry fine grained silica sand from 0.348 to 0.584 W/m.K (c. 70% increase) over a similar range of dry density.

Compared to the FEA, the time taken for the inferred geo-CTR to stabilise is somewhat longer, at 18 to 24 hours compared to about 12 hours (Figure 8). This is most probably due to the differing thermal properties assigned in the numerical analysis, compared to those of the materials used in the test. To reduce the uncertainty in the derived geo-CTR, the calibration of the thermocouples and heat flow sensors to a higher level of accuracy is essential, as small fluctuations in the temperature or heat flux readings will have a major impact on the calculated geo-CTR.

The test method in its current configuration does not consider the effect of possible moisture movement in the soil or concrete, induced by thermal gradients, Hutcheon (1958) [20]. It is also possible that thermally-induced water convection could occur near the geo-contact in saturated granular soils. This is an issue common to all existing methods for measurement of the thermal conductivity of geo-materials. Future studies will examine the use of imaging technologies or probes, Lekshmi et al (2014) [21] that might allow alterations in moisture content to be measured and its effect on the inferred geo-CTR to be quantified.

4. CONCLUSIONS

Despite being identified as a potential issue, very little appears to have been done to understand heat flow behaviour at geo-contacts, i.e. where manmade elements interface with the ground. Recent numerical studies investigating the behaviour of energy geostructures have identified the need to introduce a geo-contact thermal resistance (geo-CTR), in order to better reproduce the field behaviour of thermal response tests on energy piles.

This study has proposed a laboratory method for evaluating the geo-CTR which recognises that lateral heat losses are inevitable when imposing a heat flux through two solid materials, even if care is taken to isolate the test samples. Numerical analyses have been employed to demonstrate that a better estimate for the geo-CTR is obtained when the heat flow at the interface is measured directly.

Proof of concept testing on a dry, medium sand has shown that the methodology works and that in these materials, the geo-CTR is sensitive to the density of the soils and is at the lower end of the values suggested in other studies. Based on Figure 2, this would imply that in this particular case of a dry silica sand in contact with a limestone aggregate based concrete, the impact of the geo-CTR on energy geostructure operation and behaviour is likely to be small.

Ongoing studies are attempting to understand further the influence of soil and concrete mineralogy, initial state, contact roughness, moisture condition and other parameters on the geo-CTR, and to develop suitable models to describe the observed response in numerical analysis. By better understanding the impact of the geo-CTR on heat exchange with the ground, it is expected that more reliable predictions of thermal performance and thermo-mechanical interactions will be obtained, improving the efficiency and reducing the risks associated with the use of energy geo-structures in the future.

Acknowledgements

This work was initially developed within the scope of the research grant UID/ECI/04625/2013 financed by CERIS (Civil Engineering Research and Innovation for Sustainability), and continued under the PhD program of the second author (SFRH/BD/128845/2017) and the DEEPCOOL research project (PTDC/ECI-EGC/29083/2017) both funded by the Foundation for Science and Technology (FCT), Portugal. The authors are grateful for the financial support of the two institutions.

REFERENCES

[1] Yovanovich MM (1999) Thermal Interface (Joint) Conductance and Resistance. http://mhtlab.uwaterloo.ca/courses_old/ece309/notes/conduction/cont.pdf (last accessed 03 July 2018)

[2] Beier RA and Smith MD (2002) Borehole thermal resistance from line-source model of in-situ tests. ASHRAE Transactions, **108**(2): 212-219

[3] Svec O.J., Goodrich L.E., Palmer H.L. (1983) Heat transfer characteristics of in-ground heat exchangers, Energy Research, **7**(3):265-278

[4] Hellström G (1991) Ground Heat Storage: Thermal analysis of duct storage systems. PhD, Lund University http://portal.research.lu.se/portal/files/6178678/8161230.pdf (last accessed 3 July 2018)

[5] Wang L, Liu H, Pang Z, Lv X (2016) Overall heat transfer coefficient with considering thermal contact resistance in thermal recovery wells. International Journal of Heat and Mass Transfer, 103(Dec.): 486-500

[6] Thomas HR and Rees SW. (1999) The thermal performance of ground floor slabs – a full scale in situ experiment. Building and Environment **34**(2): 139-164

[7] ISO 6946 (2007) BS EN ISO 6946:2007 Building components and building elements - Thermal resistance and thermal transmittance - Calculation method. BSI

[8] Al-Temeemi AA and Harris DJ. (2003) The effect of earth-contact on heat transfer through a wall in Kuwait. Energy & Buildings, **35**(4): 399-404

[9] Qi, He. (2015) Thermal Performance of the Energy Geotechnical Structures. PhD Thesis, University of Cambridge

[10] Cecinato F, Piglialepre R, Loveridge F and Nicholson D. (2016) Numerical analysis of thermal cycling during a multi-stage energy pile thermal response test. Proc. 1st Intl. Conf. on Energy Geotechnics, Kiel, Germany, pp. 593-600

[11] Freitas Assunção, R.M. (2014). Thermal and thermal-mechanical analysis of thermo-active pile foundations, MSc thesis, Instituto Superior Técnico, University of Lisbon, 100 pages

[12] Xian Y., Zhang P., Zhai S., Yuan P., Yang D. (2018) Experimental characterization methods for thermal contact resistance: A review, Applied Thermal Engineering 130(February): 1530–1548

[13] Madhusudana C.V. (2000) Accuracy in thermal contact conductance experiments – the effect of heat losses to the surroundings, Int. Comm. Heat Mass Transfer 27(6): 877-891

[14] Low JE, Loveridge FA and Powrie W (2017) Error analysis of the thermal cell for soil thermal conductivity measurement. Proceedings of the Institution of Civil Engineers - Geotechnical Engineering **170**(3): 191-200

[15] Mondal S., Padmakumar G.P., Sharma V., Singh D.N. and Baghini M.S. (2016) A methodology to determine thermal conductivity of soils from flux measurement, Geomechanics and Geoengineering, **11**(1): 73-85, doi: 10.1080/17486025.2015.1020346

[16] Asif M., Tariq A., Singh K.M. (2019) Estimation of thermal contact conductance using transient approach with inverse heat conduction problem, Heat and Mass Transfer 55(11): 3243–3264

[17] Shojaeefard M.H., Goudarzi K., Mazidi M.Sh. (2009) Inverse heat transfer problem of thermal contact conductance estimation in periodically contacting surfaces, Journal of Thermal Science 18(2): 150–159

[18] Bourne-Webb, P.J., Bodas Freitas, T.M., Assução, R.M. (2016). Soil-pile thermal interactions in energy foundations, Geotechnique, **66**(2): 167-171

[19] Alrtimi A., Rouainia M. and Haigh S (2016) Thermal conductivity of a sandy soil, Applied Thermal Engineering **106**(August): 551–560

[20] Hutcheon W.L. (1958) Moisture flow induced by thermal gradients within unsaturated soils, Proc. of the 37th Annual Meeting of the Highway Research Board, http://onlinepubs.trb.org/Onlinepubs/sr/sr40/sr40-012.pdf

[21] Susha Lekshmi S.U., Singh D.N., Shojaei Baghini M. (2014) A critical review of soil moisture measurement, Measurement 54(August): 92-105, https://doi.org/10.1016/j.measurement.2014.04.007